ICCM22 MELBOURNE AUSTRALIA

TWENTY-SECOND INTERNATIONAL CONFERENCE ON COMPOSITE MATERIALS (ICCM22)

CARBON FIBER/POLYETHER ETHER KETONE RIVETS FOR FASTENING COMPOSITE STRUCTURES

C. Absi, N. Alsinani, P. Assi, A. Bureau, S. Dupont, E. Dimas and L. Laberge Lebel*

Advanced Composite and Fiber Structure laboratory (ACFSlab),
Research Center for High Performance Polymer and Composite Systems (CREPEC),
Polytechnique Montreal, 2900 Edouard-Montpetit, Montreal, QC, Canada, H3T 1J4

* LLL@polymtl.ca

Keywords: Fasteners, Rivets, Composite, Thermoplastic, PEEK

ABSTRACT

Composite materials are used for their high specific properties in modern aircraft structures. Joining these composite components brings new challenges. First, the composite cannot support the high located loads during the deformation of a metallic rivet, traditionally used to joint metallic structures. Mechanical fastening using titanium bolts is the most used joining method in the aerospace industry. However, this solution presents many drawbacks with regards to its weight, lightning strike hazard, and cost. To overcome these problems, an innovative assembly technology using carbon fiber/thermoplastic composite rivets was developed. Carbon/polyetheretherketone (C/PEEK) rods are pultruded and cut in short length blanks. The blank is heated, using Joule effect, above the melting temperature of the thermoplastic resin. It is then molded in situ, i.e, into the laminates to be joined. The materials similarity eliminates the galvanic corrosion and the electromagnetic shielding issues. The riveting parameters are controlled to ensure the joint quality and repeatability. C/PEEK blanks were used to join carbon/epoxy laminates and steel adherends. Testing showed mechanical properties higher than typical aluminum rivets in aluminum adherends. With these advantages, the technology could be applied in the next generation of aircraft structures.

1 INTRODUCTION

The use of thermoplastic composite rivets for composite structure fastening has been developed in the late 70's [1]. The technology used a shank and tube with caps, bonded together in the joint. While the technology was promising in terms of cost, weight and mechanical properties, it lacked in reliability. The bonded between the two pieces rivet was considered unreliable [2]. The alternate solution, titanium fasteners bolted-in composites structures, is still in use today. Nowadays, some studies are revisiting the topic [3, 4]. However, instead of bonding a two-part fastener, it is proposed to deform a thermoplastic composite rod into the joint hole by applying localized heat and pressure. This renewed interest is probably due to the democratization of composite materials for structural applications in the automotive and aerospace industries. Among other advantages, the weight gain compared to metallic fasteners is attractive when considering the huge quantities of fasteners in modern composite civil aircraft. A process recently developed used cylindrical rivet blanks of carbon fiber reinforced thermoplastic composites [5]. The blanks are cut from rods made by pultrusion [6]. These blanks were heated by Joule heating to reach process temperature in a composite joint. The cylindrical rivet blank was then deformed using a dedicated, semi-automated tooling. The temperature reached into the composite laminates did not affect their mechanical properties [3, 7]. Carbon reinforced polyamide (C/PA) riveted joints compared advantageously to traditional aluminum fasteners. However, the C/PA rivet properties at elevated temperature are not suited for aerospace applications. The riveting process must be attempted with thermoplastic composites retaining their mechanical properties up to 121°C hot/wet condition [8]. Carbon reinforced polyetherimide (C/PEI) blanks were also riveted in carbon fiber reinforced epoxy (CFRP) adherends [9]. These riveted joints showed a slightly improved performance compared to the C/PA rivets. Carbon reinforced polyetheretherketone (C/PEEK), a semi-crystalline polymer composite

with a glass transition temperature (Tg) of 143 °C, show great potential for this application. The objective of this study was to further develop and demonstrate the riveting process for C/PEEK blanks

2 MATERIALS

Table 1 describes the commingled C/PEEK yarns used to manufacture unidirectional composite rods. The commingled yarns (Concordia fibers) were made of 12K (AS4, Hexcel) carbon fibers and PEEK (151G, Victrex). The nominal fiber volume content of the commingled yarns was 56%.

Parameter	*Unit*	*PEEK*	*AS4 carbon fiber*
Glass transition (Tg)	°C	143	-
Melting temperature (Tm)	°C	343	-
Processing Temperature (Tp)	°C	360-420	-
Solid density [10, 11]	g/cm^3	1.30	1.79
Melt density [10]	g/cm^3	1.18	-
Melt viscosity [10]	Pa.s	[130, 300]	-
Tensile strength [10, 11]	Mpa	[105, 110]	4412
Tensile modulus [10, 11]	GPA	4.1	231

Table 1. Properties of the AS4 and PEEK fibers.

Fasteners were riveted in steel and CFRP adherends. The steel adherends were with 4.77 mm thick 4142 steel plates. CFRP adherends were made of 8HS/Epoxy (CYCOM 5276-1, CYTEC Solvay Group) prepreg with a [0/45]3S stack up. The laminate thickness was 5.1 mm. The laminate was cured in an autoclave in accordance with the manufacturer's recommendation. The epoxy Tg was 188 °C. Thick steel and CFRP adherends were used to limit bending deformation during shear testing that give rise to out-of-plane loads. Adherends were cut to produce double fastener shear coupons per NASM1312-4 standard. The holes were drilled at 4.76 mm without countersink.

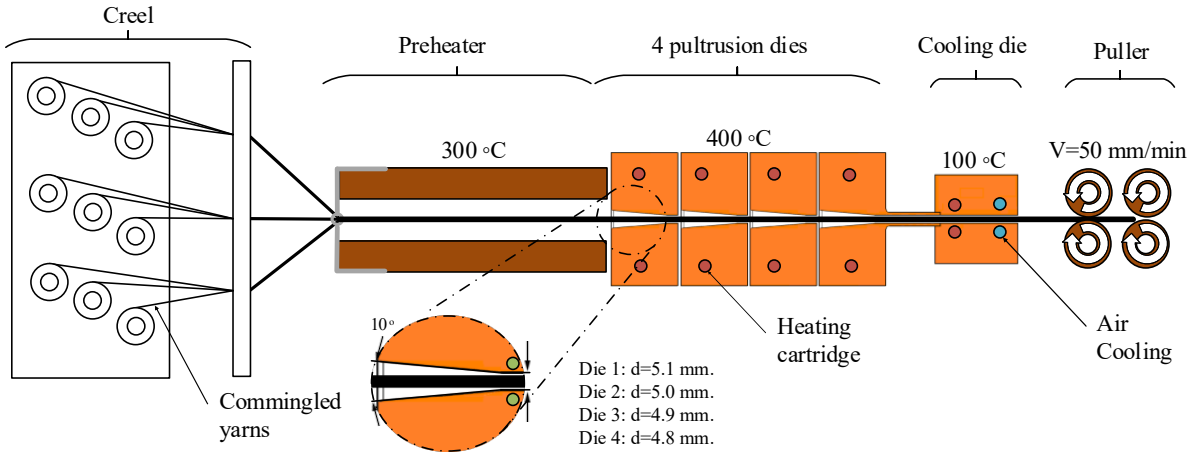

Figure 1. A schematic of the multi-die pultrusion system used in this study. The pultrusion system includes, a creel, a pre-heater, four pultrusion dies cooling die and a pulling system.

3 EXPERIMENTAL

3.1 Pultrusion of C/PEEK rods

C/PEEK rods having 4.76 mm were produced using thermoplastic pultrusion. Figure 1 shows the schematic for the pultrusion system used in this study. The pultrusion apparatus included a creel, a preheater, four-pultrusion dies, a cooling die and a pulling system. The creel carried 21 bobbins with each bobbin containing one commingled yarn. The final fiber volume fraction of the rods (*Vf*) was 56%.

The preheater was a 300-mm-long contactless preheater with an inner diameter of 12 mm. Note that all four pultrusion dies had a conical cavity with a 10° tapered angle followed by a 6.35 mm straight cylindrical cavity. The diameter of each die's cylindrical exit was 5.13, 5.00, 4.90 and 4.76 mm respectively. On the close-up view in Figure 1, the green circles represent the typical control thermocouple location in the pultrusion dies. A 31 mm long thin-walled tube with a closed circular section was protruding from the final pultrusion die. The tube`s tip point was inserted in the cooling die inlet on 3 mm with a RC5 medium running fit. Thickness of the thin wall tube was 1.59 mm. The remaining of the cooling die was at the same internal diameter than the cooling tube, i.e., 4.76 mm.

3.2 Riveting process

The riveting tooling and process are described in Figure 2. Figure 2a shows the main parts of the tooling. Each side had a similar tooling configuration. The external tubes were the bucking tool sockets, made of stainless steel. The top side was actuated by a 1 kN electrical linear actuator (KK6005C-200A1-F3, Hiwin) while the bottom side was fixed. The intermediary cylinders were the bucking tools. The bucking tools were Al2O3 ceramic tubes having an internal diameter of 4.76 mm and an external diameter of 9.5 mm. Stainless-steel plunger rods of 4.76 mm in diameter slid within the AL2O3 tubes. These plungers also served as electrodes. The two bucking tools and rams were also actuated using 1kN linear actuators (KK6005C-200A1-F3, Hiwin).

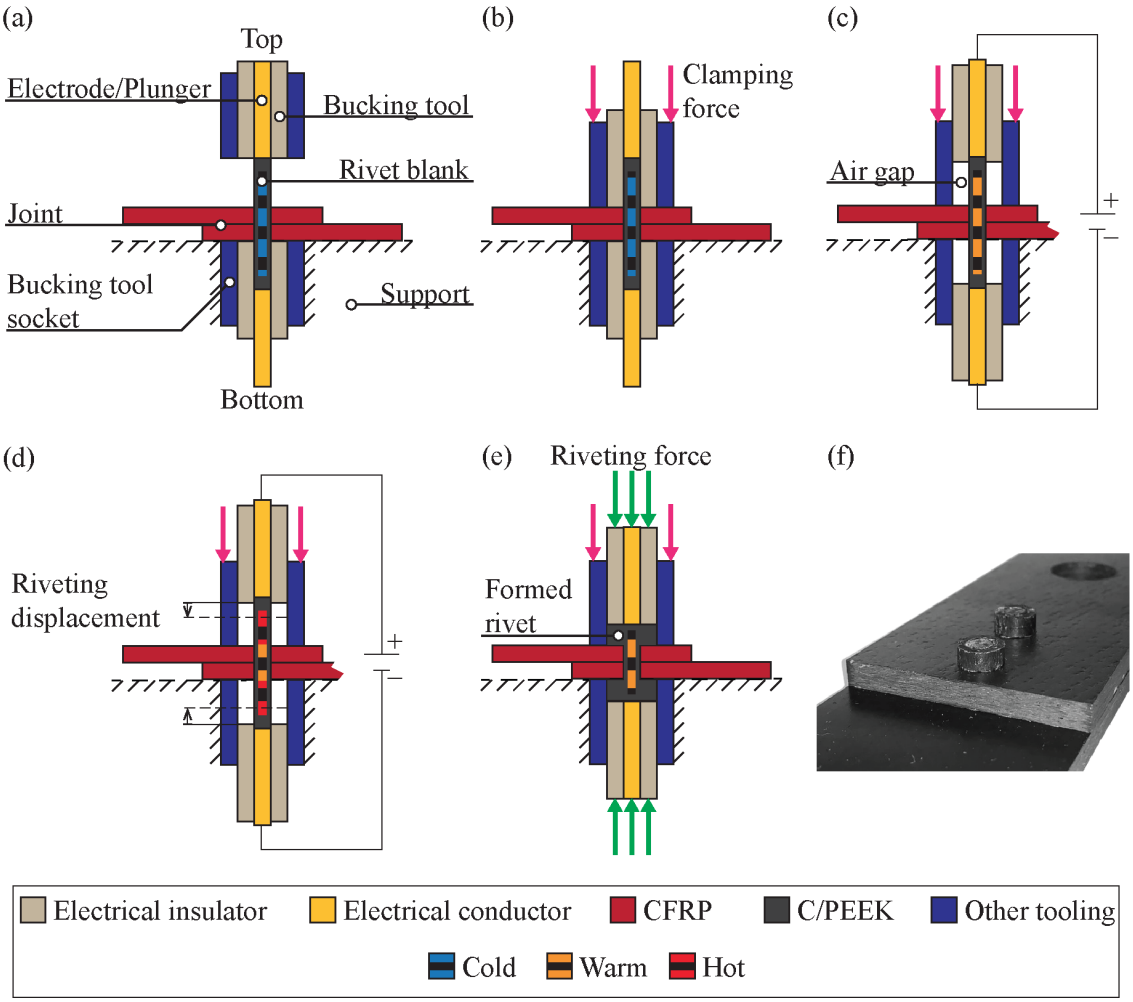

Figure 2. Riveting process: (a) Tooling description. (b) Rivet blank installation. (c) Rivet blank heating. (d) Rivet formation. (e) Cool down. (f) Typical riveted double fastener shear coupon per NAS1312-4.

At first, the riveting machine was set to initial conditions and the blank was installed in the joint. The tooling was then closed onto the joint in order to hold the adherends tightly (Figure 2b). The bucking tool sockets were used to keep the joint tight during the whole process. Once the rivet blank was installed, the bucking tools were retracted in order to create isolating air pockets for the heat to be generated in air-exposed areas (see Figure 2c). Heat was produced by Joule effect using a targeted 150 W constant power electrical current for 17 seconds. A 1 mm offset was kept between the bucking tools and the plungers in order to keep the blank straight during heating and future steps. After 15 seconds of heating, the bucking tools and plungers compressed the blank in order to form the rivet (Figure 2d). This compression was displacement driven at a speed of 230 mm/s to reach the nominal rivet head dimension. Heating was then stopped at 17 seconds. Simultaneously, the plungers and bucking tools applied a total pressure of 4.9 MPa to ensure consolidation while the rivet cooled by dissipating heat in the tooling and adherends (Figure 2e). After a 10 seconds cooling time, the tooling was opened to reveal the riveted joint (Figure 2f). The process duration was 27 seconds from the beginning of the heating stage to the opening of the tooling.

3.3 Mechanical testing

The rivets shear strength was measured according to the NASM1312-4 standard for the double fastener shear configuration. Five coupons were tested for steel and CFRP adherends using a universal tensile testing machine (MTS, Insight) equipped with a 50 kN load cell. A constant displacement rate of 0.5 mm/min was applied.

4 RESULTS AND DISCUSSION

4.1 Pultrusion of rivet blanks

Figure 3a shows the microscopic image of pultruded C/PEEK. The microscopic image is showing a circular cross-section, with insignificant void content. Figure 3b shows a microscopic image with higher magnification. The fibers look well-spread and the impregnation level appears excellent since no voids can be seen. It is likely that the cooling assembly prevented any voids that can occur from deconsolidation to form during cooling. Thermal deconsolidation occurs in thermoplastic composites when the pressure is removed prematurely during the cooling process [12-14]. Figure 3c shows the pultruded C/PEEK rods. The rods look solid with a shiny surface. The circular cross-section and the shiny surface finish may have been caused by the cooling-induced shrinkage during the cooling process. Due to the shrinkage, the final rod diameter was ~ 4.65 ± 0.03 mm. The rods were cut into blanks of 44.9 ± 0.1 mm in length.

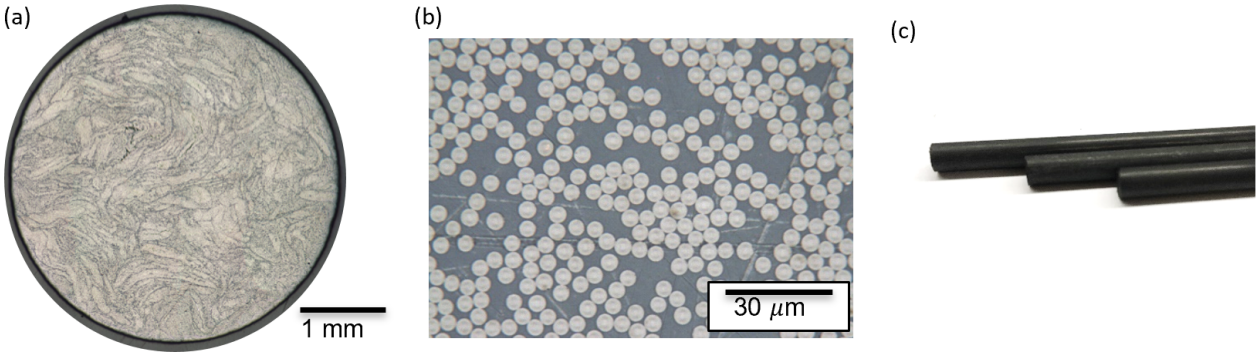

Figure 3. (a) The microscopic image of pultruded C/PEEK. The microscopic image is showing a circular cross-section with insignificant void content. (b) A microscopic image with higher magnifications. The fibers look well-spread and the impregnation level appears excellent as no voids can be seen. (c) The pultruded C/PEEK rods. The rods look solid with a shiny surface.

4.2 Riveting process characterization.

Figure 4 shows the riveting process characterization. The progress of the riveting can be tracked by,

$$Progress = Vnf / V(t) \quad (1)$$

Where *Vnf* is the final nominal volume (see Figure 4b) of the rivet head. The final nominal volume of the rivet heads was 317 mm^3. *V(t)* is the volume of the cavity enclosed by the tooling during the process duration. The start volume at *V(0 seconds)* is shown at Figure 4a. The measured applied power is shown at Figure 4c and compared to the nominal value of 150 W. The data was averaged for 10 rivets forming on each steel and CFRP coupons (20 rivets total). It is seen that the power increased to reach 150W during the first 10 seconds and stabilized for the remaining 7 seconds of the heating step. This gradual increase is attributed to the PID control of the electrical source. Figure 4d-e show the riveting process progress for the top and bottom heads, for both adherend materials. It is seen that as soon as the displacement is applied, at 15 seconds, the rivets quickly deform to reach a progress of around 100% in less than two seconds. This indicates that the PEEK polymer was melted due to the Joule heating of the carbon fibers.

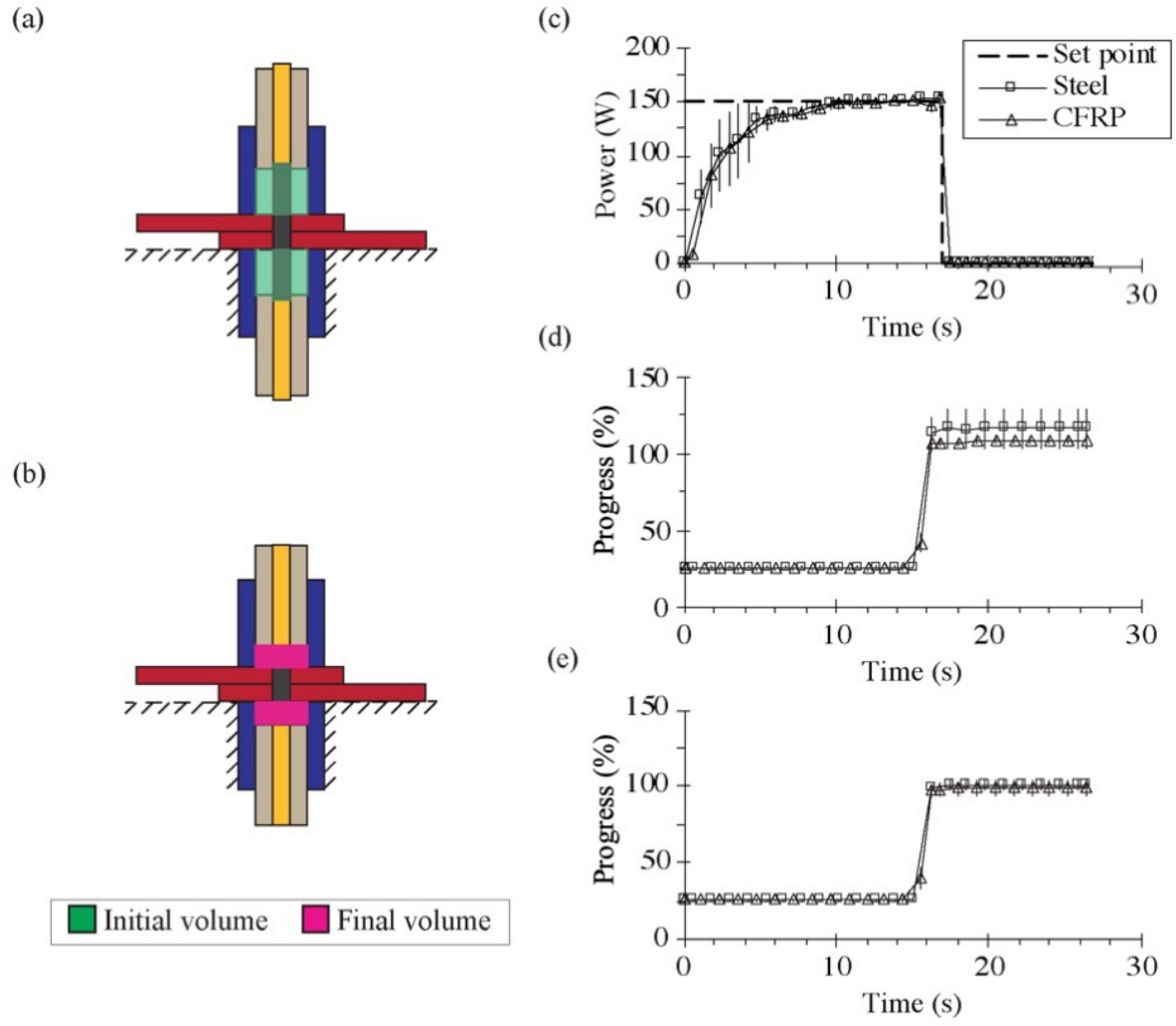

Figure 4. Process progress tracking: (a) initial volume before when buking tools are opened before heating starts. (b) Final nominal volume of rivet cylindrical heads. (c) Evolution of the electrical power applied between to the rivet. (d)-(e) top and bottom forming process progress. The progress percentage at process start was ~25% due to the given initial volume inside the riveting tooling (see (a) and equation 1).

It should be noted that the progress of the top rivet head, for the CFRP joints stabilized to a value of 107% (see Figure 4d). This means that the *V(t)* decreased to a value smaller than the final nominal volume *(Vnf)*. This could be attributed to the slight compression deformation of the gaps in the CFRP adherends. Since *V(t)* is calculated with the position of the tooling, a slight downward offset would overestimate the volume reduction. Nonetheless, the characterization of the riveting process indicates a fast and repeatable process.

4.3 Mechanical testing

Figure 5 shows the mechanical characterization of the steel and CFRP joints. Note that the load/displacement curves were corrected to remove the variations in the initial portion of the curve (see Note 17 in ASTM D5961). The load displacement/curves, presented at Figure 5a, show a different mechanical behavior from the different adherend material. The steel curve shows a stiffer behavior than the CFRP curves due to the nature of the adherend materials. Two slopes can also be seen on the steel curve. When the load reaches around half of the ultimate load, the slope increases indicating an increase in joint stiffness. This repeatable behavior will be explained in future investigations. Once the max load is reached, the load quickly drops, indicating a shear failure of the rivet without bearing deformation of the steel adherends. This is confirmed by the observation of a typical broken rivet, presented at Figure 5b, showing a net failure at the rivet mid-plane. The CFRP curve shows a typical mechanical response from a bearing failure. An offset of 2% was applied on the initial joint stiffness slope to find the 2% offset bearing load. The 2% offset was calculated with respect to the displacement at max load. It is seen that after this 2% offset bearing load, the load continues to increase to reach a maximum and then lowers until final rupture. Another indication of the bearing failure is seen at Figure 5d. The hole surface is broken since it is subjected to the compressive loads applied by the rivet shank. Once bearing failure started, the rivets rotated in the joint and were then subjected to tensile loading. The fastener rotation can be seen at Figure 5c. The final fracture of the rivets was a shank head separation due to tensile loads. A typical ruptured head can be seen at Figure 5d. The hole at the center of the rivet head indicates that the weak point of the head is located inside its core.

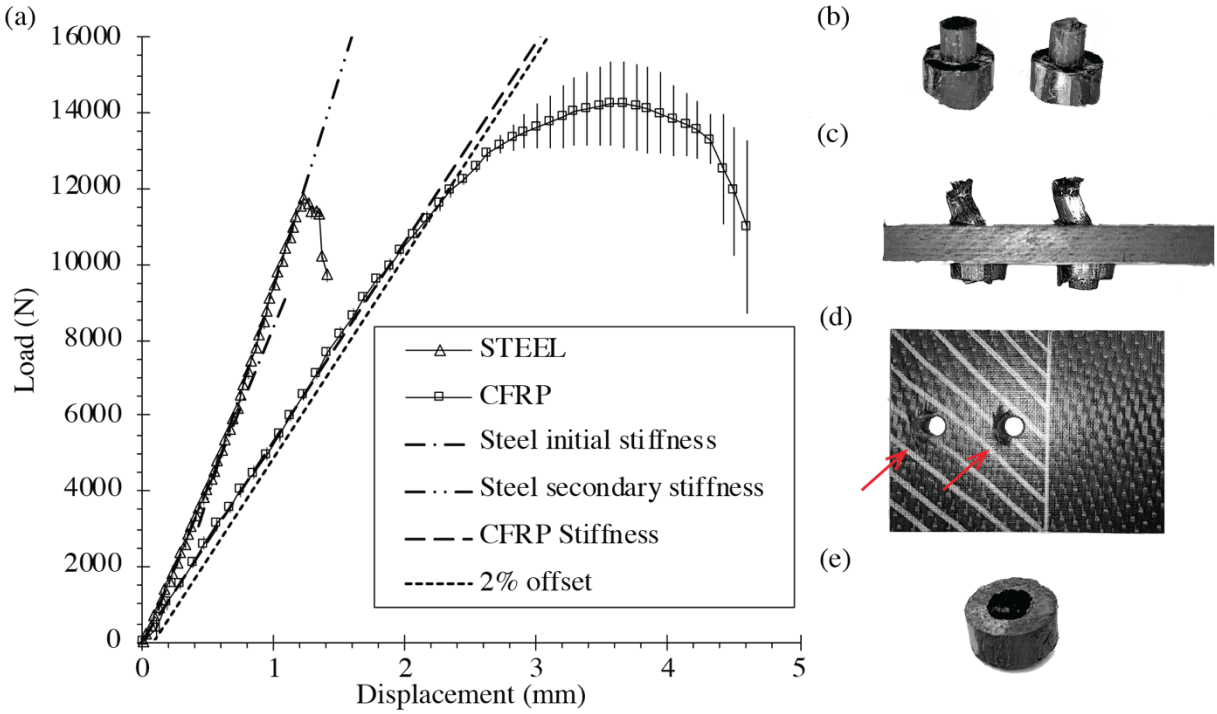

Figure 5. Mechanical characterization of the riveted joints. (a) Load/displacement response of the steel and CFRP riveted joints. (b) Mid-plane failure steel joints rivets. (c) Sideview of a failed CFRP joint with indication of fastener rotation. (d) Top view of a failed CFRP coupon with indication of bearing failure. (e) Typical tensile failure at the connection between the shank and the head from CFRP joints.

The measured mechanical properties per single rivet are shown in Table 2. The 2% offset bearing load was only reported for the CFRP joints since the exhibited a bearing failure. The apparent shear strength was calculated using the hole diameter of 4.76 mm. Peek loads and apparent shear strength at peak load are also reported. All the reported apparent shear strengths are higher than comparable aluminum aerospace grade rivets. The Mil-Hdbk-5 reports an apparent shear strength of 283 MPa for 7050-T73 rivets of 4.76 nominal diameter in Clad 7075-T6 adherends of similar thickness [15]. It is also worth mentioning that the apparent shear strength per fastener at peak load is higher than every other thermoplastic composite rivet tested in our previous studies. The C/PA rivets exhibited a strength of 313 ± 24 MPa [3]. The C/PEI rivets strength was 347 ± 23 MPa [9]. The strength increase is therefore 30% compared to C/PA rivets and 17% compared to C/PEI rivets. This increase is attributed to the improvements in process parameters and the PEEK polymer having higher mechanical properties.

Adherend Material	***2% offset bearing load (N)***	***Apparent shear strength at 2% offset load (MPa)***	***Peak load (N)***	***Apparent shear strength at peak load (MPa)***
4142 Steel	-	-	6065 ± 308	339 ± 17
CFRP	5793 ± 52	323 ± 3	7284 ± 370	407 ± 21

Table 2. Mechanical properties of the tested joints.

4 CONCLUSIONS

This study demonstrated that C/PEEK rivets can be installed in steel and CFRP joints by molding them using Joule heating and pressure. The riveting process duration, from the start of the heating phase to the demolding was 27 seconds. The process showed excellent repeatability since the rivet shape was similar for each instance. The average ultimate mechanical joint strength, of 7284 ± 370 N per rivet, was higher than for previously studied C/PA and C/PEI rivets. Future studies will improve process parameters to further reduce the riveting process duration.

ACKNOWLEDGEMENTS

The authors would like to thank Bombardier, Pultrusion Technique, NSERC (CRDPJ488387-15) and Prima Quebec (R10-009) for financing this research project.

REFERENCES

[1] Poullos, M., *Manufacturing Technology for Low-Cost Composite Fasteners, Final Report, Phases I and II*, 1979, Report No. AFML-RR-79-4044, Wright-Patterson Air Force Base, Ohio.

[2] Poon, C., *Litterature review on the design of composite mechanically fastened joints*, 1986, Report No. NAW-AN-37, NRC No. 25442, National Aeronautical Establishment, NRC, Ottawa.

[3] Fortier, V., J.-E. Brunel, and L. Laberge Lebel, *Fastening Composites Structures using Braided Thermoplastic Composite Rivets.* Journal of Composite Materials, 2019. **In Press, MS no JCM-19-0139**.

[4] Ueda, M., N. Ui, and A. Ohtani, *Lightweight and anti-corrosive fiber reinforced thermoplastic rivet.* Composite Structures, 2018. **188**: p. 356-62.

[5] Laberge Lebel, L. and V. Fortier, *Apparatus and methods for installing composite rivets,* PCT/IB2018/051448, filed on March 9, 2017

[6] Lapointe, F. and L. Laberge Lebel, *Fiber damage and impregnation during multi-die vacuum assisted pultrusion of carbon/PEEK hybrid yarns.* Polymer Composites, 2019. **40**(S2): p. E1015-E1028.

[7] Pouliot Laforte, L. and L. Laberge Lebel, *Thermal analysis and degradation of properties in carbon fiber/epoxy laminate riveting at high temperatures.* Polymer Testing, 2018. **67**: p. 205-212.
[8] Sloan, J., *Composites 101: Fibers and Resins*. Periodical Composites 101: Fibers and Resins, 2016. [Retreived 2018/06/17 from: https://www.compositesworld.com/articles/composites-101-fibers-and-resins]
[9] Fortier, V., F. Lessard, and L. Laberge Lebel, *Fastening Composite Structures Using Carbon Fiber/Polyetherimide Rivets*, in *Canada-Japan Workshop on Composites*. 2018: Takayama, Japan. p. 29-36.
[10] Victrex High Performance Polymers. *Victrex PEEK 150G/151G datasheet,* [Retreived 2019-06-27 from: http://www.victrex.com/~/media/datasheets/victrextds150g-151g.pdf.%5D]
[11] Hexcel Product Data Sheet. *HexTow AS4 carbon fiber,,* [Retreived 2019-06-27 from: http://www.hexcel.com/user_area/content_media/raw/AS4_HexTow_DataSheet.pdf]
[12] Ageorges, C., L. Ye, and M. Hou, *Experimental investigation of the resistance welding of thermoplastic-matrix composites. Part II: optimum processing window and mechanical performance.* Composites Science and Technology, 2000. **60**(8): p. 1191-1202.
[13] Beehag, A. and L. Ye, *Role of cooling pressure on interlaminar fracture properties of commingled CF/PEEK composites.* Composites Part A: Applied Science and Manufacturing, 1996. **27**(3): p. 175-182.
[14] Brzeski, M. and P. Mitschang, *Deconsolidation and its interdependent mechanisms of fibre reinforced polypropylene.* Polymers and Polymer Composites, 2015. **23**(8): p. 515-524.
[15] DoD, *MIL-HDBK-5, Metallic materials and elements for aerospace vehicule structures* 1998.